Supplemental Materials

Molecular Biology of the Cell

Goliand et al.

Supplementary Information

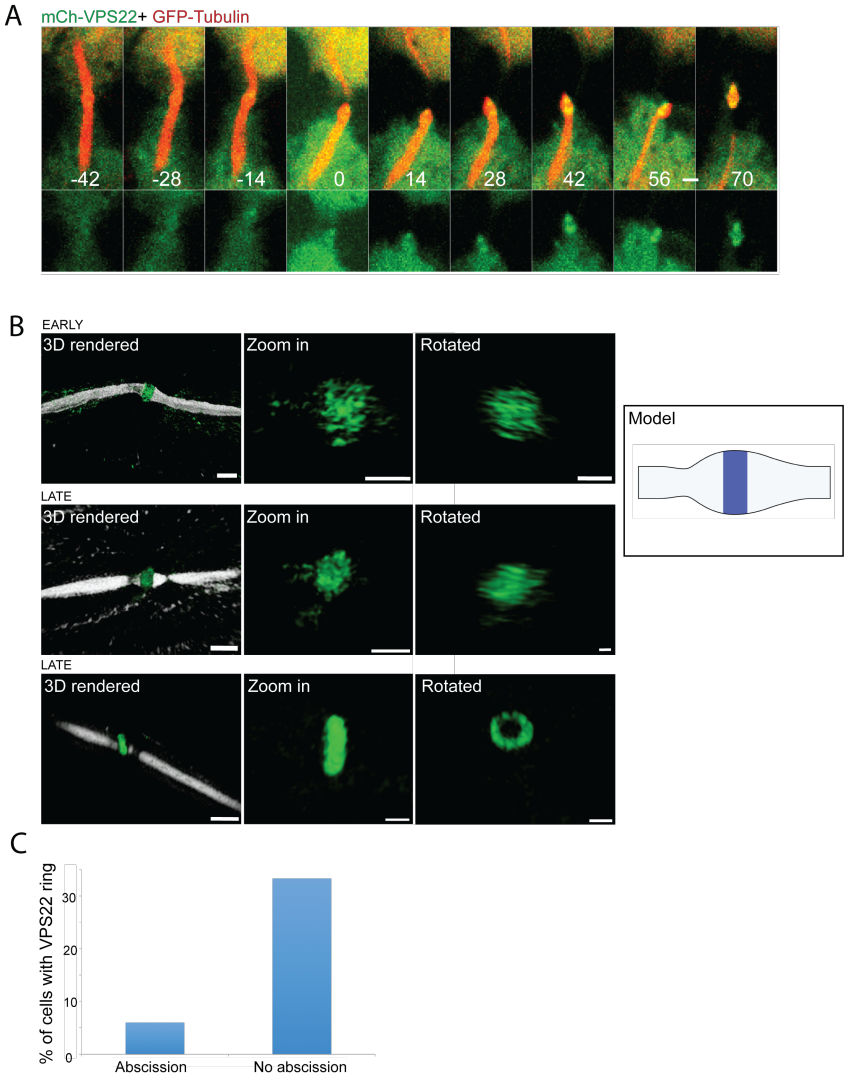

FIGURE S1

Figure S1: Recruitment of the ESCRT II protein VPS22 to the intercellular bridge during cytokinesis.

(A) Live-cell imaging of MDCK cells undergoing cytokinesis reveals recruitment of VPS22 to the intercellular bridge.

Cells expressing low levels of mCherry-VPS22 together with GFP-tubulin were imaged using a spinning-disk confocal microscope at 7 minutes intervals. Top,

overlay of VPS22 (green) and microtubules (red). Bottom, VPS22 signal alone (abscission was set at time 0 minutes, see also Supplemental video 4, n = 7, Bar, 2 μm).

(B) Spatial organization of VPS22 at the intercellular bridge.

MDCK cells expressing GFP-VPS22 were fixed, stained with anti–α-tubulin antibodies, and imaged by SIM. Early and late bridges were distinguished based on the diameter of the intercellular bridge at the constriction site.

Each panel shows from left to right: a 3D reconstruction of an overlay of VPS22 (green) and tubulin (white) in intercellular bridges (bar, 2 μm); a zoomed-in, 3D rendered image of the protein structure alone (bar, 1 μm); a zoomed-in, 3D rendered image of the protein structure rotated 90° (bar, 1 μm); schematic model for VPS22 organization at the intercellular bridge based on SIM measurements. Top and middle panels, early and late stages of cytokinesis, VPS22 concentrates in diffused pattern localized to the dark zone (n=14). Bottom panel additional organization pattern observed for VPS22 in late intercellular bridges. Instead of forming a diffused pattern, VPS22 concentrates in one ring localized to the center of the dark zone. Ring diameter: 1.48 ± 0.07 μm; ring thickness: 0.42± 0.11 μm (n=4).

(C) VPS22 ring formation is associated with abscission failure. Percentage of cells exhibiting VPS22 ring structures at the center of the intercellular bridge in normal and in abscission delayed cells (n=68).

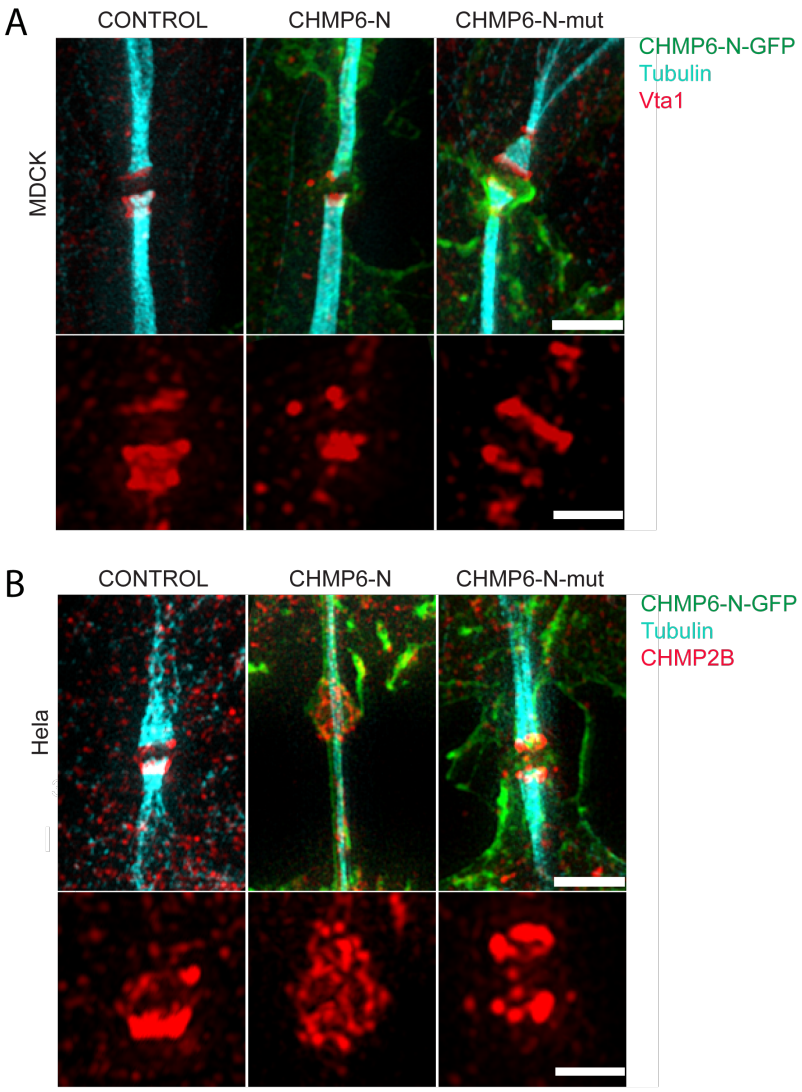

Figure S2

Figure S2. VTA1 and CHMP2B fail to properly organize at intercellular bridges of cells expressing CHMP6-N-GFP.

(A) Spatial organization of the VPS4 interacting protein VTA1 in MDCK cells. MDCK cells were fixed, stained with anti–α-tubulin and anti-VTA1 antibodies and imaged by SIM. Each panel shows intercellular bridges of (from left to right): naive cells, cells transfected with CHMP6-N-GFP and cells transfected with CHMP6-N-mut-GFP. Shown are maximum intensity projections. Top, overlay of

CHMP6-N-GFP/ CHMP6-N-mut-GFP (green), VTA1 (red) and tubulin (blue) (Bar, 2 μm). Bottom, zoomed in image of VTA1 alone (Bar, 1μm). VTA1 nicely organizes in two rings at the rims of the dark zone and is localized to the constriction sites in both naive cells and in cells expressing CHMP6-N-mut. In cells expressing CHMP6-N, however, VTA1 arrives to the intercellular bridge but fails to form high ordered structures.

(B) Spatial organization of CHMP2B in HeLa cells. HeLa cells were fixed, stained with anti–α-tubulin and anti-CHMP2B antibodies, and imaged by SIM. Each panel shows intercellular bridges of (from left to right): naive cells, cells transfected with CHMP6-N-GFP and cells transfected with CHMP6-N-mut-GFP. Shown are maximum intensity projections. Top, overlay of CHMP6-N-GFP/ CHMP6-N-mut-GFP (green), CHMP2B (red) and tubulin (blue) (Bar, 2 μm). Bottom, zoomed in image of CHMP2B alone (Bar, 1 μm). As expected, CHMP2B nicely organizes in two rings at the rims of the dark zone and is localized to the constriction sites in both naive cells and in cells expressing CHMP6-N-mut. In cells expressing CHMP6-N, however, CHMP2B arrives to the intercellular bridge but fails to form high ordered structures; instead it forms a diffused pattern at the center of the bridge.

Video 1: Dividing MDCK cells expressing low levels of mCherry-CHMP6 together with GFP-tubulin.

Cells were imaged using a spinning disk confocal at 7 minutes intervals. Shown are maximal intensity projections. CHMP6, green; tubulin, red.

Video 2: Dividing MDCK cells expressing low levels of GFP-VPS36 together with mCherry-tubulin.

Cells were imaged using a spinning disk confocal at 5 minutes intervals. Shown are maximal intensity projections. VPS36, green; tubulin, red.

Video 3: Dividing MDCK cells expressing low levels of GFP-VPS36 together with mCherry-tubulin.

Cells were imaged using a spinning disk confocal at 5 minutes intervals. Shown are maximal intensity projections. VPS36, green; tubulin, red.

Video 4: Dividing MDCK cells expressing low levels of mCherry-VPS22 together with GFP-tubulin.

Cells were imaged using a spinning disk confocal at 7 minutes intervals. Shown are maximal intensity projections. VPS22, green; tubulin, red.

Video 5: Dividing MDCK cells expressing CHMP6-N-GFP together with mCherry–tubulin.

Cells were imaged using a spinning disk confocal at 7 minutes intervals. Shown are maximal intensity projections. CHMP6-N-GFP, green; tubulin, red.

Video 6: Dividing MDCK cells expressing CHMP6-N-mut-GFP together with mCherry–tubulin.

Cells were imaged using a spinning disk confocal at 7 minutes intervals. Shown are maximal intensity projections. CHMP6-N-mut-GFP, green; tubulin, red.

Video 7: Dividing MDCK cells expressing CHMP6-N-11-52-GFP together with mCherry–tubulin.

Cells were imaged using a spinning disk confocal at 7 minutes intervals. Shown are maximal intensity projections. CHMP6-N-11-52-GFP, green; tubulin, red.

Video 8: Dividing MDCK cells expressing CHMP6-N-11-42-GFP together with mCherry–tubulin.

Cells were imaged using a spinning disk confocal at 7 minutes intervals. Shown are maximal intensity projections. CHMP6-N-11-42-GFP, green; tubulin, red.

Video 9: Dividing MDCK cells expressing CHMP6-N-1-42-GFP together with mCherry–tubulin.

Cells were imaged using a spinning disk confocal at 7 minutes intervals. Shown are maximal intensity projections. CHMP6-N-1-42-GFP, green; tubulin, red.